International Journal of Scientific Research in Engineering and Management (IJSREM)
Volume: 09 Issue: 07 | July - 2025 SJIF Rating: 8.586 ISSN: 2582-3930

Detection of Brains Tumor from MRI Images Using Convolutional Neural Network VGG19 Model

Pooja Sharma {Pooja179sharma@gmail.com},
Prof. B.L.Pal Assistant Professor Computer Science Engineering
Mewar University Chittorgarh(Rajasthan)

Abstract

Precise and automatic using imaging techniques that use magnetic resonance (MRI) to detect brain tumours remains a formidable challenge owing to the tumours' unusual shapes, diverse sizes, and intricate locations. Current methodologies frequently encounter challenges related to inadequate segmentation precision or restricted generalizability in classification endeavours. Although deep learning demonstrates significant potential, several frameworks concentrate exclusively on either segmentation or classification, resulting in insufficient diagnostic insights. An integrated system is urgently required to concurrently detect and define tumours with high precision and clinical reliability. We provide a hybrid DL system in this research that integrates the VGG19 architecture with a U-Net-based segmentation model to tackle tumour localization and binary classification. The segmentation module effectively delineates tumour locations, whereas a distinct VGG19-based classifier differentiates between tumour and nontumor MRI slices. The suggested method achieves a perfect score on the F1 test and a classification accuracy of 1.00, surpassing benchmark models including InceptionV3, ResNet50, and EfficientNetB0. Segmentation results show that the model is successful with a Dice Similarity Coefficient of 0.8509 and an IoU score of 0.7411 accurate tumour border delineation. This work's originality is in the incorporation of high-resolution spatial features from VGG19 into a cohesive dual-task framework, accompanied by a thorough assessment of both pixel-level and image-level tasks. This dual-stage architecture overcomes shortcomings in previous investigations by guaranteeing reliable tumour recognition and delineation, positioning it as a potential tool for AI-assisted diagnostics in neuro-oncology..

Keywords—*Brain Tumor Detection, MRI Classification, Semantic Segmentation, VGG19, U-Net, Deep Learning, Medical Image Analysis, Dual-Task Framework, Dice Score, IoU, Computer-Aided Diagnosis.*

I. INTRODUCTION

One of the most important areas of image processing to identify brain abnormalities from MRI images is brain tumor detection[1]. A number of image processing and machine learning algorithms are used to process the MR.I images. Pixel by pixel, the image processing techniques analyze the images to forecast how they will change. In order to forecast the changes, image processing often uses a variety of mathematical studies, clever strategies, and supervised and unsupervised algorithms [2]. To extract the pertinent information from the edge, the segmentation procedure needs more work. However, the accuracy of bra.in tumor recognition is reduced because the current approaches do not focus on the edge information. To increase the accuracy of brain tumor identification, researchers employ clever techniques and segmentation processes. In order to improve the entire detection process, this chapter addresses the layout of the brain tumor and classification approach.

According to [3], a brain tumor is an aberrant development of cells in the brain that impairs brain function. Tumors can be classified as either benign or malignant. Primary and secondary tumors are the two forms of these tumors. While secondary tumors develop outside the brain, known as metastasis, primary tumors have occurred in the brain [4]. The symptoms of brain tumors vary depending on the size of the tumor. Symptoms typically include headaches, seizures, vomiting, eyesight issues, and mental abnormalities. Patients frequently experience difficulties doing their everyday tasks, including walking, speaking, and feeling, which leads to the unconsciousness stage.

Types of Brain Tumour

Primary Tumor

As previously mentioned, brain tumors can be classified as either primary or secondary [5]. The brain, which is the trusted source of brain cells, brain membranes, nerve cells, and glands in the pineal, is where the original brain tumor begins. The main tumors are either benign or malignant. Adults typically suffer from primary tumors of gliomas and meningiomas. Glial cells produced the glioma tumor [6]. The cell maintains the structure of the nervous system, nourishes it, eliminates dead neurons, and purifies cellular waste. The three types of glioma tumors are oligodendroglia tumors (found in the frontal and temporal lobes), glioblastomas (found in brain tissues), and astrooytic tumors (found in the cerebnun). Additionally, bum.ans infects the following different types of primary malignancies [7].Pineal glandtumor Pituitary tumor , Maligmmt (primary central nervous system lymphomas) , Craniopharyngiomas , Ependymomas , Menmgiomas ,Schwannomas.

Meningiomas are more common in women than in men among the several types of primary brain tumors. Schwannoma tumors have impacted both men and women; the location and severity of the tumor determine its complications. The tumor's growth, location, and size all affect how aggressive it is.

Secondary Tumour

Different types of brain cancer are caused by secondary brain tumors [8]. The process by which brain tumors travel from one area of the body to another is called metastasis. Numerous cancers, including skin, lung, breast, and kidney cancers, are brought on by secondary brain tumors. Since the secondary brain tumor spreads throughout the body, it is always regarded as malignant.

1.2 Risk factors of Brain Tumour

The brain tumorrisk factors are listed as follows [9]

- Family history
- Age
- Chemicalexposure
- Radiation exposure
- Chickenpox histmy.

Diagnosis of Brain Tumor

Imaging techniques, including Magnetic Resonance Imaging (MRI) and Computed Tomography (CT), are employed to detect brain tumors [10]. The imaging techniques detect the brain processes and activities utilized to forecast alterations in brain

activities. Additionally, biopsies are utilized to eliminate the sick tissues from the brain. The MRI aids in predicting the brain's chemical profile that delineates the lesion on the MRI image. The Positron Emission Tomography (PET) method is employed to detect the recurrence of a brain tumor. These images are utilized to precisely diagnose brain tumors and classify brain images as normal or malignant. When a patient is diagnosed with a brain tumor, the optimal therapeutic approach is contingent upon the tumor's location, size, and the patient's overall health. According to the American Cancer Society (ACS) publication (Rock et al. 2020), in 2022, 25,050 individuals were diagnosed with a malignant brain tumor (10,880 females and 14,170 males). Experts analyze the acquired brain images utilizing methods and technologies to identify the brain tumor. MRI pictures are employed to detect cerebral abnormalities among the diverse modalities of medical imaging [11]. The MRI pictures possess numerous advantages. including elevated spatial resolution, comprehensive study of soft tissues, functional brain measurement, absence of hazards, and simplicity in assessing cerebral alterations. The aforementioned advantages are the primary rationale for choosing MRI for brain tumor detection. The sampled brain MRI images are depicted in Figure 1.

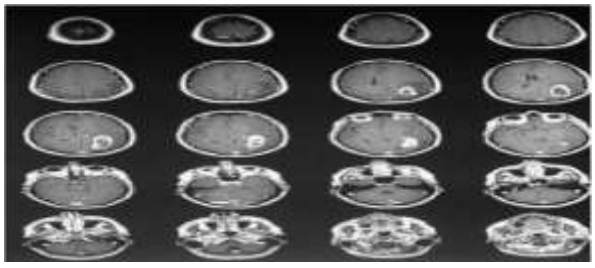

Figure 1 MRI Images of Brain

The MRI images are transmitted to the automated tumor identification system, facilitating earlier tumor detection. The comprehensive brain tumor detection procedure is illustrated in the section below.

Deep learning for medical image analysis

Medical image analysis is using deep learning to identify and diagnose conditions like cancer. To precisely detect patterns and categorize images, deep learning models are trained on vast collections of annotated medical images. In the end, this could result in better patient outcomes by increasing the speed and accuracy of medical diagnostics [12]. But issues like ethics, data privacy, accuracy, and dependability need to be addressed. Research is still being done to create deep learning algorithms for medical image

processing that are more effective and efficient. The earlier detection method employs several stages, including processing, data extraction, segmentation, picture collecting, feature selection, and categorization [13]. Each phase has a designated function utilized to forecast the brain tumor. The general framework of the automatic brain tumor detection technique is illustrated in Figure 2.

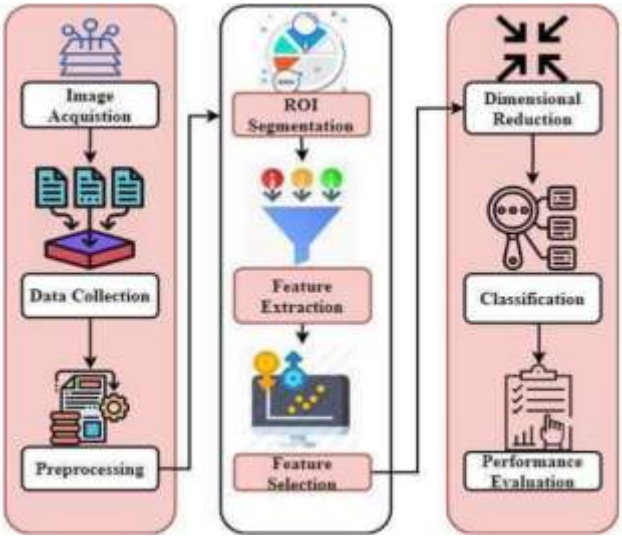

Figure 2: General Structure of Brain Tumour Detection

The classification's basic diagram is shown in Figure 1.2. Most medical experts would steer clear of the manual detection of tumor indicators and the recruitment of prospective medications for this option because brain tumors are lethal. Using computer vision algorithms to analyze medical images is the most modern and risk-free approach. It includes gradedetennining algorithms for tumor diagnosis and short lln.ages taken with different tools. These techniques can be modified for tumor segmentation, showing how the tainted areas of the images are separated from the healthy ones. Effective and prompt therapy of a patient depends on the early detection and classification of a brain tumor. As a result, techniques for brain tumor categorization (BTC) or computer-assisted diagnosis (CAD) are developed , which help radiologists identify and categorize tumor types more accurately [14]. The automated techniques for identifying, classifying, and segmenting brain tumors are a tremendous benefit to humanity since they eliminate the need for invasive surgery (biopsy).Deep learning research indicates that the quantity of available data significantly affects the system's accuracy.

Image Preprocessing

The initial phase of the automatic brain tumor identification procedure is image processing, during which the image quality is enhanced [17]. The pre-processing phase eliminates extraneous pixel information, mitigates distortion, and enhances image attributes to optimize image quality. To enhance image quality, this stage is occasionally referred to as the lowest level of abstraction. The processing is conducted in four methods: pixel brightness adjustment, geometric transformation, picture filtering, and image restoration. In pixel brightness, image pixels are altered according to pixel attributes. The input pixels are consistently analyzed in relation to neighboring pixels, and the contrast and brightness of the pixel are adjusted correspondingly. Enhanced brightness and contrast in pictures are extensively utilized for medical image processing and clinical decision-making [18]. The brightness transformation procedure comprises numerous operations, including gamma correction, sigmoid stretching, and histogram equalization. In geometric transformation, pixel positions are continuously analyzed, and the pixels are altered without impacting the image's color. This method reduces the geometric distortion that

occurs during image capturing. Typically, distortion, scaling, and rotation techniques are employed on the image to enhance its quality [19]. The geometric transformation is executed in two phases: spatial interpolation and grey-level interpolation. The spatial transformation is accomplished by physically reorganizing the image pixels. In grey level interpolation, grey levels are assigned to the modified images. The subsequent crucial pre-processing step involves filtering, wherein image attributes are augmented by extracting pertinent information. Several strategies for noise removal in images encompass low-pass filtering, high-pass filtering, Laplacian filtering, and Gaussian filtering [20].

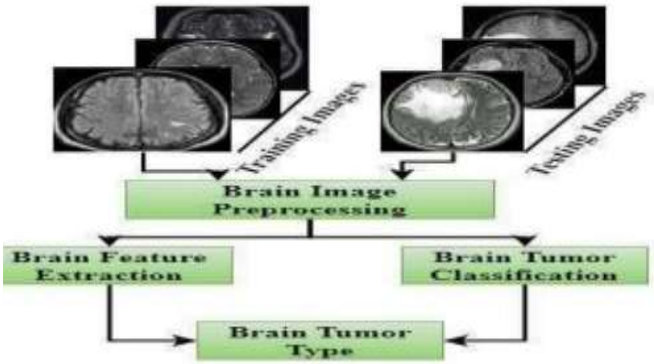

Figure 3: Image Pre – Processing

Image Segmentation:

The second phase, image segmentation, involves dividing images into sub-images [21]. The segmentation procedure decreases computational complexity during picture analysis. The segmentation procedure assigns labels to the segmented regions to identify individuals, objects, and other critical features within the image. The picture segmentation procedure is extensively utilized in the medical area and object detection to facilitate essential decision-making. The segmentation method employs bounding box techniques to enhance region identification. The segmented region is utilized to decrease inference time and enhance recognition accuracy. The segmentation process is a crucial component of image-processing applications such as facial recognition, autonomous vehicle detection, medical imaging, and item detection.

II . LITERATURE REVIEW

[23]Brain tumors exhibit rapid cell growth and can be deadly if not detected early. Despite advancements, precise segmentation and classification remain challenging due to variations in tumor location, size, and shape. This research compiles extensive MRI-based detection literature and introduces both statistical and AI-driven methods, including neural networks and transfer learning. It also highlights preprocessing techniques like component extraction and augmentation, alongside system evaluation using standard datasets and morphological analysis.[24]The foundational principle of brain tumor detection involves distinguishing aberrant tissue from healthy brain matter. MRI-based medical imaging has enabled automation of core tasks like extraction, segmentation, and classification. Despite this, the variability in tumor morphology—shape, size,and location—continues to challenge computer-aided diagnostic systems. Researchers have explored numerous segmentation and classification approaches, critically evaluating their strengths, limitations, and technical constraints. This survey delves into these methodologies, outlining strategies, preferences, and future considerations in MR imaging for brain tumor identification.[25] This study explores deep learning (DL) models for brain tumor identification using MRI scans. One model classifies images into normal vs. abnormal, while the other targets three tumor types: meningiomas, gliomas, and pituitary tumors. Researchers utilized two public datasets—one with
3064 images, the other with 140. The primary model is a 23 Layer convolutional neural network (CNN), trained with extensive data. To address overfitting on the smaller dataset, they enhanced the architecture by integrating VGG16 through supervised learning. Comparative analysis with prior research reveals superior performance, with classification accuracies of 97.8% and 100%, surpassing existing models.[26] This research emphasizes the critical need for early detection of brain cancer, as survival and treatment planning on timely diagnosis. Manual techniques are tedious, making automated, computer-assisted methods increasingly valuable despite occasional errors. The paper presents a segmentation algorithm that uses the Fig share dataset and combines UNet architecture with ResNet50, achieving an impressive IoU score of 0.9504.To enhance classification accuracy across different tumor classes, the system integrates reinforcement learning, transfer learning, and evolutionary algorithms. A performance comparison of several CNN models—MobileNetV2,InceptionV3, ResNet50, DenseNet201, and NASNet Revealed NASNet as the most accurate, achieving up to 99.6% accuracy, with others ranging from 91.8% to **93.1%**.[27] Brain tumors arise from uncontrolled cell growth and can be fatal if not diagnosed early. Despite meaningful progress, segmentation and classification of brain tumors remain difficult due to wide variation in tumor size, shape, and location. This literature assessment provides an extensive review of MRI-based detection techniques, exploring: Tumor Anatomy and morphological complexities Open-source datasets for training and validation,Data augmentation and feature extraction methods ,Segmentation and classification algorithms .Advanced approaches like Deep Learning (DL), Transfer Learning (TL), and Quantum Machine Learning (QML).The paper critically examines strengths, limitations, and emerging trends in the field, serving as a valuable guide for researchers and developers tackling MRI-based brain tumor identification.[28] Early detection of brain malignancies is critical, as typical tumors can grow within 25 days and become fatal in under six months without treatment. Automated MRI-based methods offer promising solutions to reduce the burden on radiologists. This study proposes a lesion segmentation framework using parameters like shape, texture, and intensity, followed by classification via Support Vector Machines (SVMs). Evaluated on three datasets—local, RIDER, and Harvard—the approach achieved high accuracy with sensitivity of 91.9%, specificity of 98.0%, and an AUC of 0.98, outperforming existing techniques in speed and reliability.[29] Brain tumors can be either malignant or benign, with malignant types accounting for roughly one-third of intracranial cases. Large tumors may compress nearby structures, impairing neurological function. Researchers are exploring liquid biopsies as non-invasive alternatives for detecting tumor biomarkers in cerebrospinal fluid or blood, such as tumor cells, IDH mutations, MGMT methylation, and microRNAs. These help track cancer progression. Common treatment strategies include surgery, radiation, and targeted therapy. Ongoing studies are investigating novel inhibitors for advanced malignancies.[30] Advanced deep learning architectures, including CNNs, Swin Transformers, and EfficientNets, were utilized for brain tumor classification. MRI scans were scaled, normalized, and augmented across four datasets, one featuring healthy brains. These preprocessed images trained models tested for specificity, accuracy, and sensitivity. EfficientNet demonstrated superior

performance—98.72% testing accuracy—and computational efficiency, making it ideal for resource-constrained settings. Swin Transformers also outperformed standard CNNs, confirming that modern DL architectures significantly enhance tumor classification accuracy.

III. METHODOLOGY

This study utilized two publicly accessible brain MRI datasets to facilitate binary classification and tumour segmentation: the BraTS-Africa dataset and the IXI dataset.

A. BraTS-Africa and IXI Dataset

The BraTS-Africa dataset was obtained from The Cancer Imaging Archive (TCIA) and compiled from six prominent diagnostic centres in Nigeria. It offers annotated MRI data for glioma patients, highlighting inclusion by incorporating African populations that are often underrepresented in medical AI databases. This dataset comprises multi-parametric scans.

Data set link:
https://www.cancerimagingarchive.net/collection/Bra

https://brain-development.org/ixi-dataset/

Image Format Unification and Conversion

Medical imaging datasets are generally preserved in volumetric formats such as NIfTI (.nii.gz), which encapsulate three-dimensional brain architecture. The BraTS-Africa and IXI datasets both underwent this change to ensure uniformity.

B. Image Resizing and Normalization

To unify input dimensions and facilitate batch processing in neural networks, all images were reduced to 256×256 pixels.

C. Label Encoding for Classification

All photos from the BraTS-Africa dataset were designated as '1' (tumour), whereas those from the IXI dataset were designated as '0' (non-tumor).

D. Data Augmentation (BraTS-Africa Dataset)

Data augmentation encompassed several changes, including horizontal and vertical flips, random rotations, zooming, and contrast modifications. Following augmentation, the BraTS-Africa dataset increased to 642 imagemask pairs, hence improving the training dataset for classification and segmentation tasks.

E. Mask Preprocessing for Segmentation

For the segmentation task, accurate annotations are preprocessing phase guarantees that the masks are precisely matched and aligned with their corresponding input images, which is essential for loss calculation and efficient model training in segmentation.

F. Train-Test Splitting

To assess model generalization and performance, the data were divided into training and testing sets in an 80:20 ratio.

G. Model Building

Architectures designed for two main objectives of the system: binary classification of MRI images into tumor and non-tumor categories, followed by precise segmentation of tumor regions from the positively classified slices.

H. Image-Level Classification Using VGG-19

A binary classifier based on the VGG19 architecture was employed to automatically identify MRI slices with potential tumors, filtering out irrelevant images before segmentation. VGG19's 19-layer design (16 convolutional + 3 fully connected layers) enables effective hierarchical feature extraction through ReLU and max-pooling.

The original top layer was replaced with a custom head: global average pooling → dense layer (128 units, ReLU) → dropout → sigmoid output. Trained using binary cross-entropy and Adam optimizer, the model's performance was assessed via accuracy, precision, recall, and F1 score, ensuring only tumor-relevant images proceed to segmentation.

Tumor Region Segmentation Using U-Net with VGG19 Encoder

After image-level classification successfully distinguishes tumor-containing slices from nontumorous cases, the subsequent phase focuses on tumor localization through pixel-wise segmentation. This step is essential for delineating the spatial extent of abnormal regions within each MRI image.

I . VGG19 Encoder

Pretrained VGG19 convolutional blocks (5 stages of 3×3 filters + ReLU + max-pooling) extract fine-grained spatial features crucial for medical imaging.

J. U-Net Architecture

U-Net's symmetric encoder-decoder layout enables pixel-wise segmentation with both global context and local precision. VGG19 serves as the encoder; the decoder uses transposed convolutions for upsampling and spatial reconstruction.

K. Decoder & Skip Connections

Upsampling layers reconstruct spatial dimensions; each is followed by convolution and batch normalization to refine outputs and suppress noise, enhanced by skip connections from the encoder.

L. Output Layer

A 1×1 convolution paired with sigmoid activation generates a binary mask classifying each pixel as tumor (1) or background (0).

M. Model Configuration Parameters

The organized framework for efficient tumour segmentation in brain MRI slices. The integration of Utilizing a VGG19 encoder, U-Net reapeds the benefits of both frameworks—profound feature extraction and accurate spatial reconstruction. All images, both input and output, are set to the same size of 256×256 to streamline preprocessing and enable pixel-wise assessment. The hardware was addressed using minimum batch size of sixteen restrictions and ensure that the model could be trained without memory overflow, while still delivering dependable gradient estimates. Sixty epochs were adequate for the model to converge without overfitting. With an exponential learning rate of 1e-4 and the Adam optimizer were selected to facilitate smooth and adaptive gradient changes. Skip connections and batch normalization are essential components of this system. Skip links link the encoder and decoder, maintaining detailed spatial information throughout layers. Batch normalization is implemented following each convolution in the decoder pathway to mitigate internal covariate shift, expedite training, and enhance

generalization. In order to do binary classification, the output layer employs sigmoid activation for each pixel, producing a mask that corresponds with relation to the supplied image's dimensions.

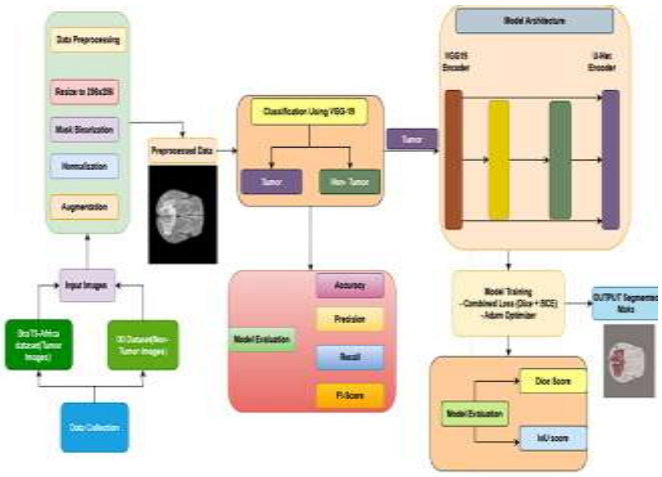

Figure 4: Flowchart

O. *Train the model*

VGG19 was trained on segmented images. The Alex Net and ResNet50 techniques are used to evaluate the suggested model's efficacy.

P. *Model Evaluation*

Model evaluation was conducted in two stages: classification and segmentation.

Q. *Classification Metrics*

To assess the performance of the VGG19-based binary image-level classifier responsible for distinguishing between tumor and non-tumor MRI slices, a comprehensive set of evaluation metrics was employed.

R *Performance Metrics*

Performance measurements from the confusion matrix, including Accuracy, Recall, Precision, and F1-score, are used to evaluate model performance.

Accuracy:

Accuracy is the proportion of participants who, out of all

$$Accuracy = \frac{TP + TN}{TP + TN + FP + FN} \quad (1)$$

Precision:

To assess an outlook's accuracy, add up all correctly predicted events .Another name for this concepts is forecast value.

$$Precision = \frac{TP}{TP+FP} \quad (2)$$

Recall:

The ratio of correct proportional to the sum of the realand false negatives

$$\text{Recall} = \frac{TP}{TP+FN} \quad (3)$$

N. Model Evaluation

Model evaluation was conducted in two stages: classification and segmentation.

IV. RESULT

The classification results demonstrate how well deep learning models differentiate between MRI scans showing brain tumours and those showing non-tumors slices. Among the evaluated models, the proposed VGG-19-based classifier achieves perfect scores across the board in terms of review criteria including recall, accuracy, precision, and F1-score —indicating exceptional reliability and zero misclassification on the test set. In contrast, ResNet50 and DenseNet121 also show strong performance, though slightly lower, while InceptionV3 records the lowest metrics among the four. These findings show how the VGG-19 model is better at correctly detecting brain Tumor patterns from axial MRI slices.

F1-Score:

The F1 score is a single score that includes precision and recall

$$\text{F1-score} = 2 * \frac{Precision * Recall}{Precision + Recall} \quad (4)$$

S. Segmentation Metrics

Dice Similarity Coefficient (DSC):

$$DSC = \frac{2TP}{2TP+FP+FN} \quad (5)$$

Intersection over Union (IoU):

$$IoU = \frac{TP}{(TP + FP + FN)} \quad (6)$$

Model	Accuracy	Precision	Recall	F1-Score
VGG-19	1	1	1	1
ResNet50	0.9545	0.9683	0.9531	0.9606
DenseNet121	0.9227	0.944	0.9219	0.9328
InceptionV3	0.8636	0.9016	0.8594	0.88

Table 2:Evaluation Metrics table for Brain Tumor classification model

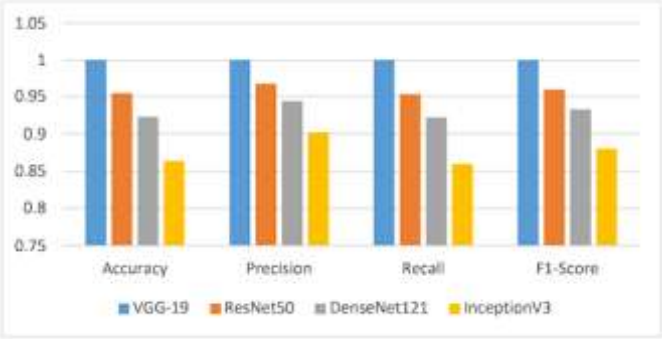

Figure 5:Comparison performance for Brain Tumor classification models

The confusion matrices for ResNet50, DenseNet121, InceptionV3, and VGG-19, evaluating their binary brain tumor classification performance. These matrices offer visual insight into each model's accuracy and misclassification trends using axial MRI slices.

From the below confusion matrix the efficacy of the DenseNet121 model, which correctly identifies 85 nonTumor and 118 Brain Tumour pictures. Nonetheless, it exhibits a marginally elevated misclassification rate relative to ResNet-50, with 7 ten false negatives and one false positive. This is results in an overall accuracy of 92.27%, indicating a decline in model resilience, particularly in the accurate classification of non-Tumor pictures. The decline in performance is also seen in the diminished accuracy (94.40%) and F1-score (93.28%) metrics relative to ResNet-50.

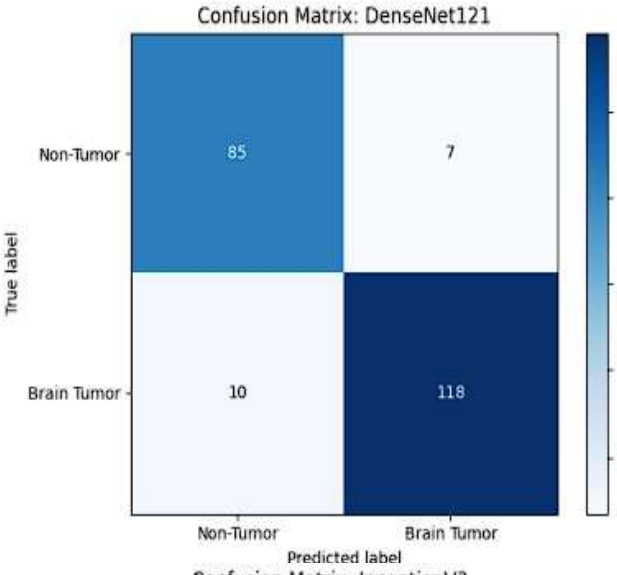

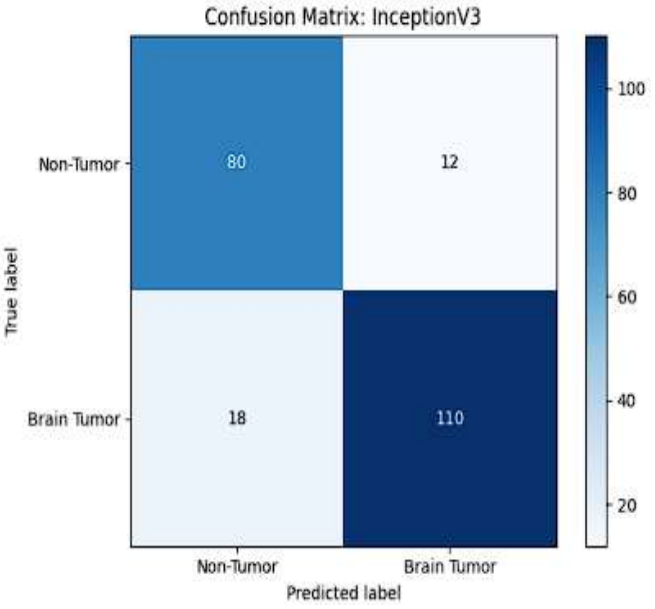

This graphical representation of matrix misunderstanding for ResNet-50 model, indicating accurate classification of 88 non-Tumor and 122 Brain Tumour photos, with 4 non-Tumor samples incorrectly categorized as Brain Tumour (false positives) and 6 Brain Tumour images misclassified as non-Tumor (false negatives). This yields a total of 10 misclassifications from 240 samples, resulting in an overall accuracy of 95.45%. Despite robust performance, especially in detecting Brain Tumour instances, the occurrence of both misclassification types suggests a considerable compromise when comparing specificity to sensitivity.

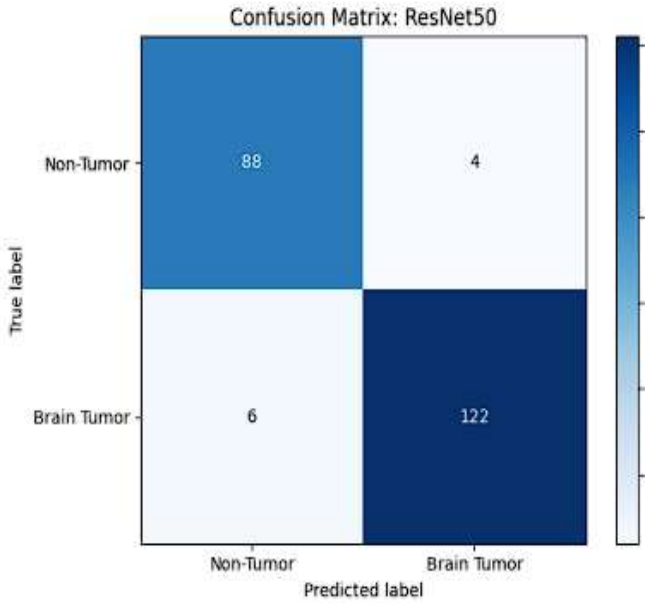

The confusion matrix for the InceptionV3 model least classification proficiency among the evaluated models. It accurately recognizes 80 non-Tumor and 110 Brain Tumour instances, but misclassifies 12 non-Tumor and 18 Brain Tumour cases, resulting in a lower accuracy of 86.36%. The increased misclassification count significantly affects the model's sensitivity and precision, leading to a reduced F1-score of 88.00%. The results indicate that InceptionV3 may have difficulty in accurately identifying the pertinent visual elements required for dependable brain tumour classification in MRI images.

This study evaluates brain tumor classification using four deep learning models—VGG-19, ResNet50, DenseNet121, and InceptionV3—based on axial MRI slices. Performance metrics include accuracy, precision, recall, and F1-score, derived from confusion matrices. **VGG-19** outperforms all models with perfect scores of **1.0000** across all criteria, proving highly reliable in distinguishing tumor from non-tumor images.

ResNet50 also performs well, achieving an F1-score of **0.9606**, while **DenseNet121** shows balanced sensitivity and precision, scoring **0.9328** in F1. **InceptionV3**, however, records the lowest performance (**F1: 0.8594**), indicating higher misclassification rates. Figure 2 visually confirms these results, with VGG-19 consistently reaching maximum values while others show dips—especially InceptionV3 in recall.

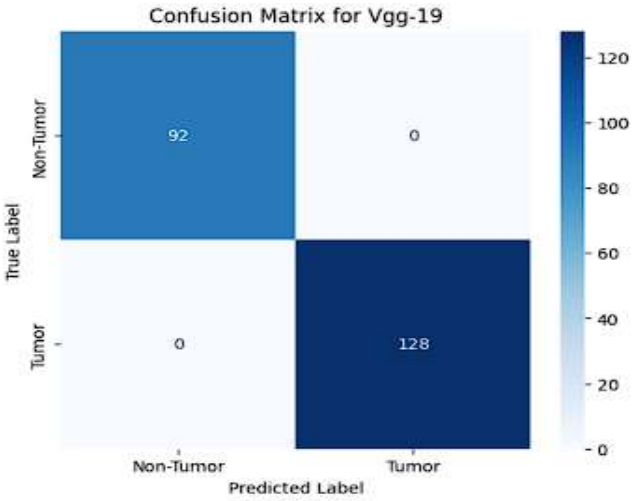

Overall, VGG-19 is validated as the most efficient and dependable binary classifier in this comparative study.

The confusion matrices indicate that ResNet-50 and DenseNet121 demonstrate robust and consistent performance with little misclassifications, however InceptionV3 exhibits inferior dependability. Conversely, the VGG-19 model distinguished itself as the top architecture for brain tumour classification in this experiment, demonstrating unparalleled performance both quantitatively and qualitatively. These findings underscore the necessity of meticulous model selection, as even minor architectural variations can profoundly affect medical diagnostic results.

ROC curves serve as valuable tools in evaluating the effectiveness of brain tumor classification models by illustrating their diagnostic accuracy across varying thresholds.

The Area Under the Curve (AUC) displays the model's ability to differentiate between non-tumor and tumour cases every classifier.

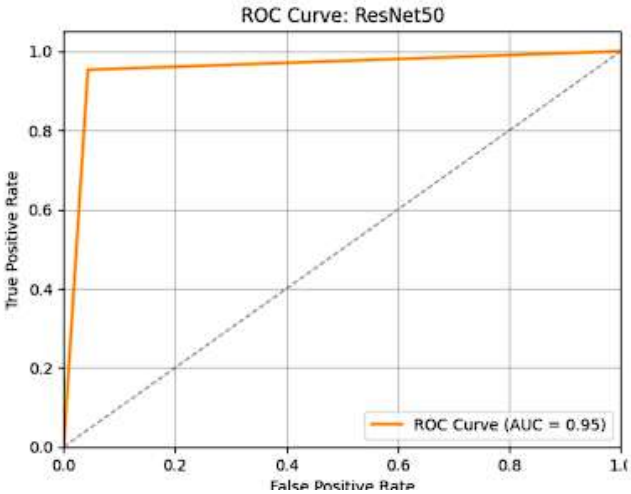

ROC curve for the ResNet50-based model, with an AUC of 0.95. The elevated AUC indicates that the model has robust classification proficiency, characterized by a comparatively relatively low rates of false positives and high rates of genuine positives. Extreme sensitivity and specificity are shown by the sharp rise of the curve towards the upper left corner, establishing ResNet50 as a dependable foundation for brain tumour identification in this research.

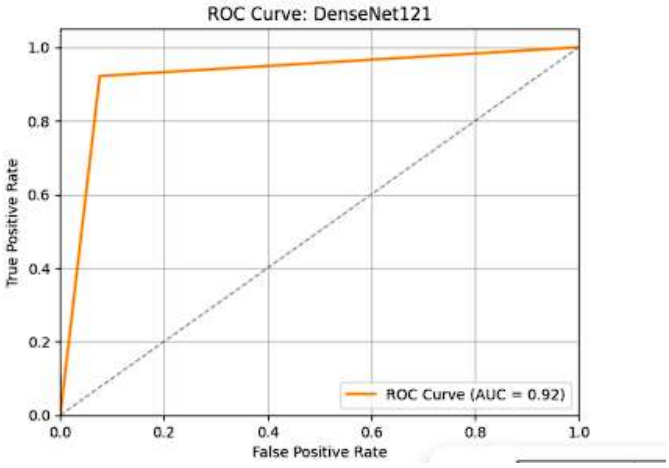

The DenseNet121-based model's Area Under the Curve (ROC), which obtained an AUC of 0.92. This figure represents adequate performance in categorization, however marginally inferior to ResNet50 and VGG19. The ROC curve demonstrates substantial sensitivity at various thresholds, affirming DenseNet121 as a formidable contender for brain tumour classification, particularly due to its densely connected architecture that enhances gradient flow and feature reutilization.

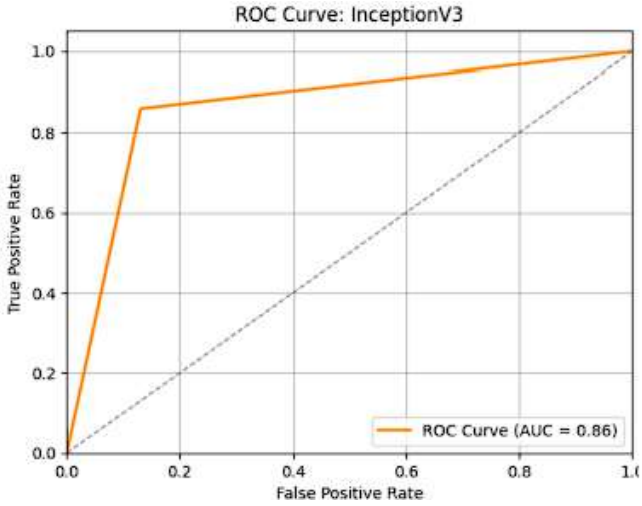

ROC curve for the model built using InceptionV3 contained the lowest AUC value of 0.86 among the assessed architectures. The curve exhibits a milder gradient relative to others, particularly in the initial segment where false positive rates are minimal. This indicates that InceptionV3 possesses comparatively diminished discriminate capability in differentiating Brain Tumour images from non-tumor images, maybe attributable to underfitting or inadequate feature extraction within the medical imaging domain.

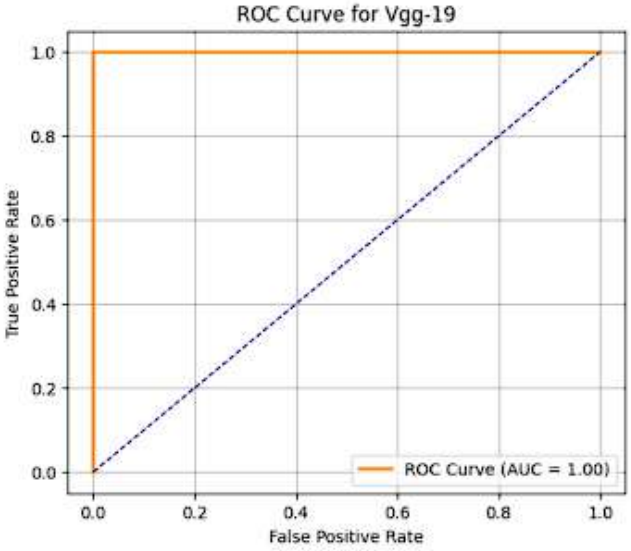

VGG19 classifier, which attains an impeccable AUC of 1.00. The ROC curve exhibits a distinct right angle in the upper left quadrant, indicative of impeccable classification efficacy. This outcome indicates that the VGG19 model, utilized as an independent image-level classifier, can efficiently and reliably distinguish between Brain Tumour cases and non-tumor instances without error. The effectiveness of VGG19 in this context is due to its rich yet consistent architecture and its capacity to preserve intricate spatial elements crucial for medical diagnosis.

The ROC study validates the superiority of simpler yet more profound convolutional networks, such as VGG19, in medical picture classification, especially in differentiating delicate brain tumour patterns.

VGG19 emerges as the most proficient classifier, attaining optimal separation performance among all models. ResNet50 and DenseNet121 exhibit strong performance, achieving AUC scores

over 0.90, which signifies substantial predictive capability. InceptionV3, although performing adequately, exhibits somewhat diminished efficacy, indicating it may not be ideal for this particular Brain Tumour categorization job. The ROC study validates the superiority of simpler yet more profound convolutional networks, such as VGG19, in medical picture classification, especially in differentiating delicate brain tumour patterns.

Segmentation Results:

This section details the quantitative assessment of the suggested segmentation framework on the test dataset, which makes use of the VGG19-U-Net architecture. It is common practice to use either the Dice coefficient or the IoU score when calculating gauge how effective medical image segmentation algorithms. Indicative of improved performance, these measures quantify the degree to which ground truth annotations and predicted segmentation maps coincide. To ensure the suggested model worked as intended, we ran comparison tests against three reference models: Vanilla U-Net, ResNet34-U-Net, and SegNet with a VGG16 backbone.

Model	IoU Score	Dice Score
VGG19-U-Net (Proposed)	0.7411	0.8509
U-Net	0.6597	0.7935
ResNet34-U-Net	0.6832	0.8124
SegNet with VGG16 Backbone	0.7016	0.8258

Table 3:Performance Metrics Table for segmentation

The segmentation efficacy of four distinct models within the context of the experimental dataset. Impressive results were achieved by the VGG19- U-Net model, which obtained a Dice coefficient of 0.7411 and an IoU of 0.8509, indicating high-quality segmentation and accurate delineation of brain tumour boundaries. Dice and the baseline Vanilla U-Net model's IoU scores of 0.7935 and 0.6597, respectively, demonstrated less overlap with ground truth masks and worse prediction accuracy.

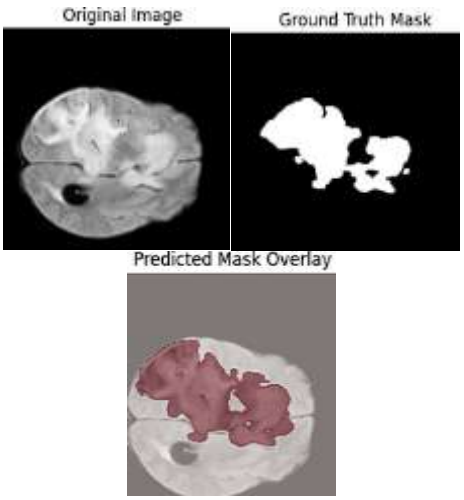

Figure 6 : Visual Comparison of Ground Truth and Predicted Tumor Masks Using the Proposed VGG19 + U-Net Model

V. DISCUSSION

Our finding show that the binary tumour classifier utilizing VGG19 demonstrated perfect performance, attaining 100% test accuracy alongside immaculate F1-scores, recall, and precision. The ROC curve corroborated this, exhibiting an AUC of 1.00, signifying flawless differentiation between Tumour and Non-Tumor groups. This exceptional performance is also evident in the confusion matrix, which exhibited no misclassifications. The VGG19-based classifier consistently surpassed other conventional deep learning classifiers, including InceptionV3, ResNet50, and EfficientNetB0, in benchmark evaluations. The VGG19 model demonstrated enhanced accuracy and recall, highlighting its enhanced ability to generalize and accurately detect tumour presence throughout the dataset. The comparative bar chart extracted from the performance metrics table clearly demonstrates the extent to which the suggested model exceeds these baselines, offering an explicit view of its competitive advantage.

Not with standing these encouraging outcomes, some constraints persist. Because A limited and targeted dataset for both model training and evaluation, the results' generalizability to larger clinical populations is restricted. An expanded, multi-center dataset would facilitate the formulation of more robust findings. The existing binary classification framework confines the model to differentiating solely between tumour and non-tumor slices. In clinical practice, the additional categorization of tumours into subtypes, including gliomas, meningiomas, and pituitary cancers, is essential for therapy planning. Furthermore, the exemplary classification measures, albeit remarkable, elicit apprehensions regarding possible overfitting to the training dataset. External validation with novel datasets is necessary to validate the model's persistence and its usefulness. In the end, the computational intricacy of the VGG19 backbone necessitates substantial memory and processing time, rendering the framework less appropriate for use in clinical settings in real time without improvement.

VI. CONCLUSION

This work introduced an automated technique that combines a U-Net model with the VGG19 to identify and segment brain tumours in magnetic resonance imaging (MRI) slices architecture. The system was developed to address two important difficulties in medical image analysis: exact tumour segmentation and precise categorization of MRI slices as tumour or nontumor. The quantitative findings indicated the superiority of the proposed model, achieving a segmentation IoU of 0.7411 and a Dice Score of 0.8509, along with a test ideal classification metric for image-level diagnostic tasks of 1.00 (accuracy, precision, recall, F1-score, and AUC). These results demonstrate the model's efficacy in identifying tumour presence and precisely delineating tumour margins. The visual validation of segmentation masks substantiates the clinical potential of the model by demonstrating consistent alignment between predicted and real tumour locations. The classification performance was evaluated against other models for deep learning, such as EfficientNetB0, ResNet50, and InceptionV3, using the VGG19-based classifier consistently surpassing all benchmarks. The performance was illustrated through both tabular and graphical comparisons, with the VGG19 model exhibiting enhanced discriminative ability in distinguishing Tumour from Non-Tumor slices. Notwithstanding these benefits, the framework possesses specific constraints, such as the reliance on a binary classification model, the potential for overfitting stemming from elevated accuracy on restricted datasets, including the computational load linked to deep structures. These problems may impede real-world adoption until rectified in subsequent trials.

Future endeavours will prioritize expanding the dataset to include a greater representative and varied group of MRI pictures, preferably sourced from several clinical centres. The model's robustness and ability to generalize will be enhanced by this.

Furthermore, the classification pipeline will be enhanced to accommodate multi-class output, facilitating the distinction among different tumour types, hence aligning more closely with clinical requirements. Advanced regularization methods and external validation mechanisms will be employed to reduce the hazards of overfitting. Ultimately, model compression methods, including pruning and knowledge distillation, may be investigated to diminish computing demands and facilitate realtime clinical implementation. The suggested framework, with these changes, possesses significant potential to function as an effective and precise instrument for computer-aided diagnosis in brain tumour investigation.

VII. REFERENCES

[1] M. Sharif, J. Amin, M. Raza, M. A. Anjum, H. Afzal, and S. A. Shad, "Brain tumor detection based on extreme learning," Neural Comput. Appl., vol. 32, no. 20, pp. 15975–15987, 2020, doi: 10.1007/s00521-019-**04679-8**

[2] A. Asokan, J. Anitha, M. Ciobanu, A. Gabor, A. Naaji, and D. J. Hemanth, "Image processing techniques for analysis of satellite images for historical maps classificationAn overview," Appl. Sci., vol. 10, no. 12, 2020, doi: 10.3390/app10124207

[3] M. Toğaçar, B. Ergen, and Z. Cömert, "BrainMRNet: Brain tumor detection using magnetic resonance images with a novel convolutional neural network model," Med. Hypotheses, vol. 134, p. 109531, 2020, doi: https://doi.org/10.1016/j.mehy.2019.109531.

[4] Z. Hu, Z. Li, Z. Ma, and C. Curtis, "Multi-cancer analysis of clonality and the timing of systemic spread in paired primary tumors and metastases," Nat. Genet., vol. 52, no. 7, pp. 701–708, 2020, doi: 10.1038/s41588-020-0628-z.

[5] T. C. Hollon et al., "Near real-time intraoperative brain tumor diagnosis using stimulated Raman histology and deep neural networks," Nat. Med., vol. 26, no. 1, pp. 52–58, 2020, doi: 10.1038/s41591-019-0715-9.

[6] J. Han, Y. Cui, B. Xu, W. Xue, S. Liu, and J. Dai, "Three-Dimensional Cell Culture and Tissue Restoration of Neural Stem Cells Under Microgravity BT - Life Science in Space: Experiments on Board the SJ-10 Recoverable Satellite," E. Duan and M. Long, Eds., Singapore: Springer Singapore, 2019, pp. 235–279. doi: 10.1007/978-981-13- 6325-2_10.

[7] S. Lee, L. Y., Cazier, J. B., Starkey, T., Briggs, S. E., Arnold, R., Bisht, V., ... & Ellis, "COVID-19 prevalence and mortality in patients with cancer and the effect of primary tumour subtype and patient demographics: a prospective cohort study," Lancet Oncol., vol. 21, no. 10, pp. 1309–1316, 2020, doi: 10.1016/S1470-2045(20)30442-3.

[8] R. K. Arvanitis, C. D., Ferraro, G. B., & Jain, "The blood–brain barrier and blood– tumour barrier in brain tumours and metastases," Nat. Rev. Cancer, vol. 20, no. 1, pp. 26–41, 2020, doi: 10.1038/s41568-019-0205-x.

[9] A. M. Lewandowska, M. Rudzki, S. Rudzki, T. Lewandowski, and B. Laskowska, "Environmental risk factors for cancer - review paper," Ann. Agric. Environ. Med., vol. 26, no. 1, pp. 1–7, 2019, doi: 10.26444/aaem/94299.

[10] S. M. Bafaraj, "Evaluation of Neurological Disorder Using Computed Tomography and Magnetic Resonance Imaging," J. Biosci. Med., vol. 09, no. 02, pp. 42–51, 2021, doi: 10.4236/jbm.2021.92005

[11] M. Talo, U. B. Baloglu, Ö. Yıldırım, and U. Rajendra Acharya, "Application of deep transfer learning for automated brain abnormality classification using MR images," Cogn. Syst. Res., vol. 54, pp. 176–188, 2019, doi: 10.1016/j.cogsys.2018.12.007.

[12] H. I. Shen, D., Wu, G., & Suk, "Deep Learning in Medical Image Analysis," Annu. Rev. Biomed. Eng., vol. 19, no. 1, pp. 221–248, 2017, doi: 10.1146/annurev-bioeng071516-044442.Deep.

[13] M. A. Khan, T. Akram, M. Sharif, K. Javed, M. Raza, and T. Saba, "An automated system for cucumber leaf diseased spot detection and classification using improved saliency method and deep features selection," Multimed. Tools Appl., vol. 79, no. 25, pp. 18627–18656, 2020, doi: 10.1007/s11042-020-08726-8.

[14] K. Muhammad, S. Khan, J. D. Ser, and V. H. C. d. Albuquerque, "Deep Learning for Multigrade Brain Tumor Classification in Smart Healthcare Systems: A Prospective Survey," IEEE Trans. Neural Networks Learn. Syst., vol. 32, no. 2, pp. 507–522, 2021, doi: 10.1109/TNNLS.2020.2995800.

[15] B. Jena et al., "Brain Tumor Characterization Using Radiogenomics in Artificial Intelligence Framework," Cancers (Basel)., vol. 14, no. 16, 2022, doi: 10.3390/cancers14164052

[16] I. Thomassin-Naggara et al., "Artificial intelligence and breast screening: French Radiology Community position paper," Diagn. Interv. Imaging, vol. 100, no. 10, pp. 553–566, 2019, doi: https://doi.org/10.1016/j.diii.2019.08.005.

[17] M. Ramamoorthy, S. Qamar, R. Manikandan, N. Z. Jhanjhi, M. Masud, and M. A. Alzain, "Earlier Detection of Brain Tumor by Pre-Processing Based on Histogram Equalization with Neural Network," Healthc., vol. 10, no. 7, pp. 1–13, 2022, doi: 10.3390/healthcare10071218.

[18] N. Heller et al., "The state of the art in kidney and kidney tumor segmentation in contrast-enhanced CT imaging: Results of the KiTS19 challenge," Med. Image Anal., vol. 67, pp. 1–39, 2021, doi: 10.1016/j.media.2020.101821.

[19] C. Tian, X. Chai, and F. Shao, "Stitched image quality assessment based on local measurement errors and global statistical properties," J. Vis. Commun. Image Represent., vol. 81, p. 103324, 2021, doi: https://doi.org/10.1016/j.jvcir.2021.103324

[20] O. Susladkar et al., "ClarifyNet: A high-pass and low-pass filtering based CNN for single image dehazing," J. Syst. Archit., vol. 132, p. 102736, 2022, doi: https://doi.org/10.1016/j.sysarc.2022.102736

[21] K. Rasool Reddy and R. Dhuli, "Segmentation and classification of brain tumors from MRI images based on adaptive mechanisms and ELDP feature descriptor," Biomed. Signal Process. Control, vol. 76, p. 103704, 2022, doi: https://doi.org/10.1016/j.bspc.2022.103704.

[22] P. Veerlapalli and S. R. Dutta, "A hybrid GAN-based deep learning framework for thermogram-based breast cancer detection," Sci. Rep., vol. 15, no. 1, pp. 1–33, 2025, doi: 10.1038/s41598-025-04676-z.

[23] S. Solanki, U. P. Singh, S. S. Chouhan, and S. Jain, "Brain

tumor detection and classification using intelligence techniques: an overview," IEEE Access, vol. 11, pp. 12870–12886, 2023.

[24] P. K. Chahal, S. Pandey, and S. Goel, "A survey on brain tumor detection techniques for MR images," Multimed. Tools Appl., vol. 79, no. 29, pp. 21771–21814, 2020.

[25] M. S. I. Khan et al., "Accurate brain tumor detection using deep convolutional neural network," Comput. Struct. Biotechnol. J., vol. 20, pp. 4733–4745, 2022.

[26] T. Sadad et al., "Brain tumor detection and multi-classification using advanced deep learning techniques," Microsc. Res. Tech., vol. 84, no. 6, pp. 1296–1308, 2021.

[27] J. Amin, M. Sharif, A. Haldorai, M. Yasmin, and R. S. Nayak, "Brain tumor detection and classification using machine learning: a comprehensive survey," Complex Intell. Syst., vol. 8, no. 4, pp. 3161–3183, 2022.

[28] J. Amin, M. Sharif, M. Yasmin, and S. L. Fernandes, "A distinctive approach in brain tumor detection and classification using MRI," Pattern Recognit. Lett., vol. 139, pp. 118–127, 2020.

[29] M. Pichaivel, G. Anbumani, P. Theivendren, and M. Gopal, An overview of brain tumor. IntechOpen, 2022.

[30] M. S. Elhadidy, A. T. Elgohr, M. El-Geneedy, S. Akram, and H. M. Kasem, "Comparative analysis for accurate multi-classification of brain tumor based on significant deep learning models," Comput. Biol. Med., vol. 188, p. 109872, 2025.